Doping Induced Tailoring in the Morphology, Band-Gap and Ferromagnetic Properties of Biocompatible ZnO Nanowires, Nanorods and Nanoparticles

Javed Iqbal[1,2,*], Tariq Jan[2], Yu Ronghai[1,3], Sajjad Haider Naqvi[4], Ishaq Ahmad[5]

Abstract: The modification of nanostructured materials is of great interest due to controllable and unusual inherent properties in such materials. Single phase Fe doped ZnO nanostructures have been fabricated through simple, versatile and quick low temperature solution route with reproducible results. The amount of Fe dopant is found to play a significant role for the growth of crystal dimension. The effect of changes in the morphology can be obviously observed in the structural and micro-structural investigations, which may be due to a driving force induced by dipole-dipole interaction. The band gap of ZnO nanostructures is highly shifted towards the visible range with increase of Fe contents, while ferromagnetic properties have been significantly improved. The prepared nanostructures have been found to be nontoxic to SH-SY5Y Cells. The present study clearly indicates that the Fe doping provides an effective way of tailoring the crystal dimension, optical band-gap and ferromagnetic properties of ZnO nanostructure-materials with nontoxic nature, which make them potential for visible light activated photocatalyst to overcome environmental pollution, fabricate spintronics devices and biosafe drug delivery agent.

Keywords: ZnO; Fe doping; Dipole-dipole interaction; Band-gap tailoring; Ferromagnetism; Cytotoxicity

Introduction

ZnO is an important group of II–VI semiconductor with the characteristics of wide direct band gap (3.37 eV), large exciton binding energy (60 meV), inexpensive and environmentally safe material [1,2]. Due to these remarkable characteristics, ZnO nanomaterials have attracted a lot of research interest in the field of science and technology [3,4]. Among ZnO nanomaterials family, the one dimensional (1D) ZnO nanostructures (such as nanowires, nanorods, nanofibers and nanotubes etc) are of special interest because of their high surface area and compatibility with the functional nanodevices. Due to these significant properties, the 1D ZnO nanostructures has found large number of applications in many devices such as nano lasers, single nanowire field effect transistor, UV blockers and detectors, power generators and gas sensors [5-9]. For all these devices, the controlled nanoscale morphological characteristics are highly desired.

[1]Laboratory of Advanced Materials, Department of Material Science and Engineering, Tsinghua University, Beijing, China
[2]Laboratory of Nanoscience and Technology, Department of Physics, International Islamic University Islamabad, Pakistan
[3]School of Materials Science and Engineering, Beihang University, Beijing, China
[4]Karachi University, Karachi, Pakistan
[5]Nanational Center for Physics (NCP), Quaid-i-Azam University, Islamabad, Pakistan
*Corresponding author. javed.saggu@iiu.edu.pk

In these days, ZnO based photocatalyst is considered to be an excellent substitute of TiO_2 to overcome the current global environmental pollution problem due to its good stability and non-toxic nature [10]. However, the large band gap of ZnO lies in the UV range, which allows for only ∼6% of sunlight to be useful for the activation of the catalyst. Therefore, a visible light activated catalyst is highly desired that can take advantage of a larger fraction of the solar spectrum and would be much more effective in environmental cleanup [11]. It has been found that the optical band gap energy of ZnO nanostructures can be effectively tailored via doping of different transitional metals (TMs) [12]. In addition, currently a lot of experimental and theoretical research is also concentrated on TM doped ZnO dilute magnetic semiconductors (DMSs) because of their room temperature ferromagnetic behavior [13]. ZnO nanostructures with tailored optical and magnetic properties may have useful applications in future spintronics devices [13]. In order to look above functionality with morphological modification, optical improvements and room temperature ferromagnetism with high T_c, Fe is supposed to be a potential candidate for doping in ZnO.

In addition, the inorganic nanostructures have an important role in biomedical sector because of their significant photocatalytic and antibacterial characteristics [14]. Among these, ZnO nanostructures are of special attention because of their cost effectiveness and established applications in health care products [15]. ZnO could also be used for drug delivery but toxicity concern is there. Bulk ZnO is considered as safe material by FDA (US Food and Drug Administration) but when reduced to the nanoscale, ZnO can develop new actions of toxicity [16].

In this work, Fe doped ZnO nanostructures including nanoparticles, nanorods and nanowires based on the soft chemistry synthetic approach have been prepared at room temperature. A series of Fe doped ZnO samples with varying Fe contents have been systematically studied. The band gap of ZnO has been dramatically reduced with the increase in Fe doping level. The morphology of doped samples shows an interesting change from 1D to zero dimension (0D). The resulting Fe doped ZnO nanostructures possess both tuned optical and magnetic properties, which will enable them for designed industrial applications. Furthermore, the cytotoxicity of Fe doped ZnO nanostructures has been studied and found to be nontoxic for SH-SY5Y Cells.

Experimental

Fe doped ZnO nanostructures have been prepared using wet chemical method as in our previous reported work [17,18]. Different analytical grade chemicals have been used for the fabrication of ultrafine nanostructures. In a typical synthesis process, 0.5 M NaOH solution prepared in ethanol as precipitating agent has been added drop by drop into molar solution of 0.05 M $Zn(NO_3)_2 \cdot 6H_2O$ with different stoichiometric ratio of $FeCl_3 \cdot 6H_2O$ at normal laboratory temperature for 1 h.

$$Zn(NO_3)_2 + NaOH \rightarrow Zn(NO_3)(OH) + NaNO_3$$
$$Zn(NO_3)(OH) + NaOH \rightarrow ZnO + NaNO_3 + H_2O$$
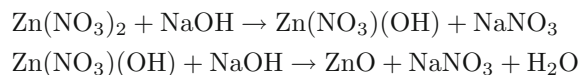
After one hour of vigorous magnetic stirring, the solution has been put into an Autoclave (Teflon vessel) and heated at 120℃ for 15 h. The precipitates have been collected, washed and then centrifuged. Finally, these washed precipitates have been dried in oven at 110℃. Different characterization techniques have been employed as were used in our previous reported work [17,18].

The SH-SY5Y cells of human being have been used as target which are commercial available at ATTC, USA. The cells have been cultured at 37℃ in DMEM medium for 48 h with in humidified environment. The colloidal solution of the synthesized nanostructures with different Fe doping level has been used against these cells. The cells cultured without the presence of these nanostructures have been used as control for comparison.

Results and discussion

Morphology and microstructure

The morphology and microstructure of these prepared crystalline samples have been carefully investigated using electron microscopy techniques. Figure 1(a), (b), (c) and (d) demonstrate the TEM, HRTEM and SAED images of Fe doped ZnO with different compositions x= 0.5%, 1%, 2% and 5% of Fe dopant, respectively. It has been interestingly found that the prepared doped samples undergo a significant morphological changes induced by the amount of Fe dopant concentrations into ZnO structure. The pure ZnO sample portrays the nanowires of length 5 μm and their growth direction is preferably oriented along c-axis. Figure 1(a) shows the morphology of $Fe_{0.5}Zn_{99.5}O$ sample, which exhibits nanowires of average length 3 μm with 40 nm of diameter. The microstructure study with HRTEM of grown nanowires shows single phase structure with the interspacing between planes of 0.22 nm and length of c-axis 0.5204 nm, which reveals that the growth direction of these nanowires is preferably oriented along (0001) as shown in Fig. 1(a). The sample with the nominal composition of x = 1% has a morphology of nanorods within the average length of 900 nm and a diameter of 90 nm as shown in Fig. 1(b). The microstructural HRTEM study of these as prepared nanorods shows that the c-axis lattice constant value is little reduced and the spacing between planes is also changed.
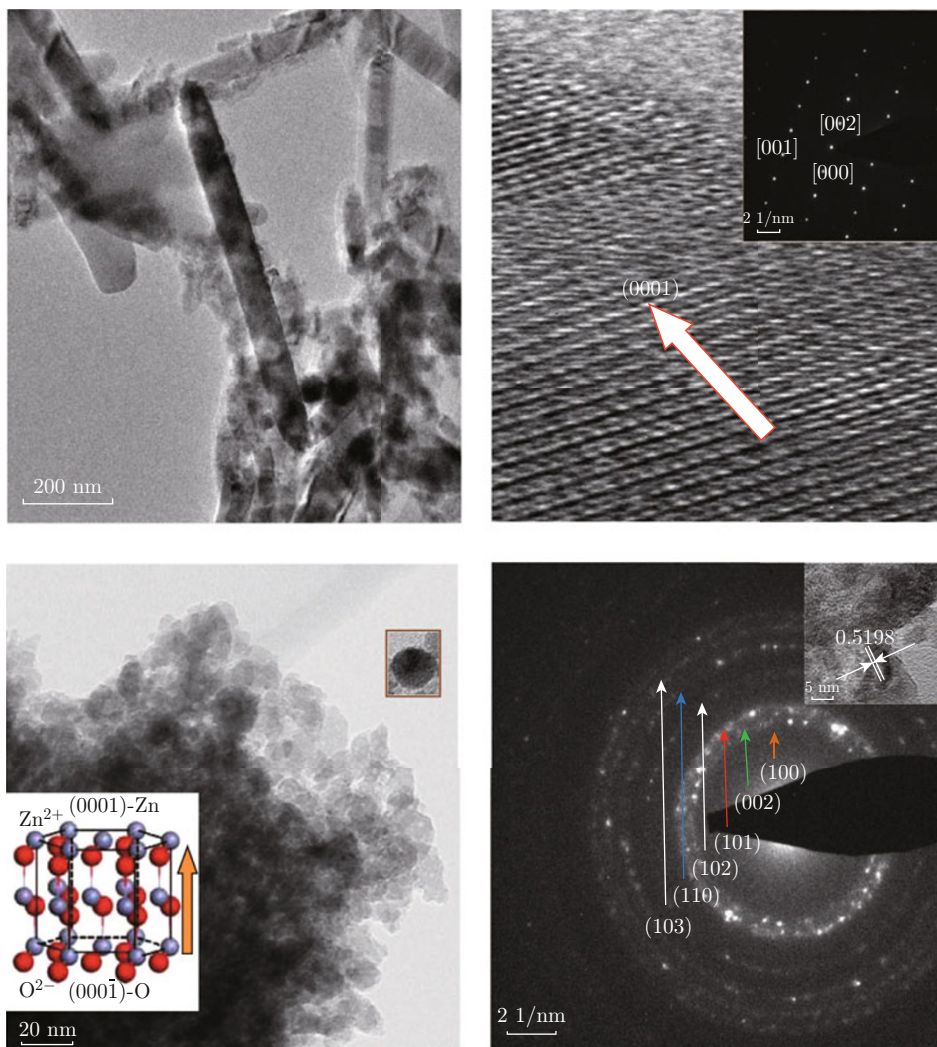
Fig. 1   TEM, HRTEM and SAED patterns of Fe (x=0.5%, 1%, 2% and 5%) doped ZnO Nanostructures.
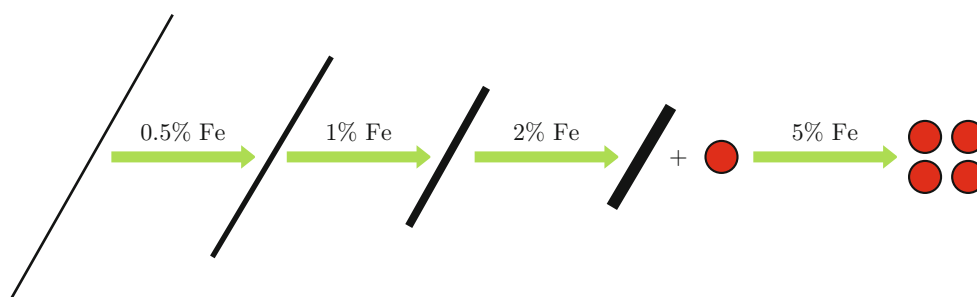
Diagram 1   Schematic drawing of Fe doping induced tailoring in the morphology

However, the absence of secondary phases can be ruled out from Fig. 1(b). With the increase of Fe doping concentration up to 2%, there are two kinds of mixed morphology consisting of nanorods and nanoparticles as shown in Fig. 1(c). The major part of morphology is nanorods, whose micro-structural investigation in high resolution shows that the growth along c-axis planes is highly influenced and the micro-structure has mixed morphology overlook. In order to confirm the structure

formation, SAED has been carried out for this sample and is depicted in the Fig. 1(c). All resolved fringes pattern of diffraction shows the single phase wurtzite structure formation. When the concentration of Fe dopant is increased up to 5%, the morphology is dramatically changed from 1D to nanoparticles as shown in Fig. 1(d). The average size of these nanoparticles lies in the range of 12 nm. The HRTEM and SAED investigations of these prepared nanoparticles demon-

strate that they are in ZnO wurtzite single phase and all selected area diffraction fringes can be indexed to hexagonal wurtzite structure as shown in Fig. 1(d). In order to make the picture of morphology change more clear, it has been noted that with the introduction of Fe into ZnO lattice, the growth along c-axis is affected and the length of nanowires and nanorods is decreased, while diameter increased, which gives the evidences of some force to hinder the growth of crystal along *c*-axis. There is overall a schematic change in the morphology with the variation of Fe doping concentration as depicted in diagram 1.

The growth mechanism of nanocrystal structure can be explained on the basis of the polar surfaces of ZnO. The hexagonal wurtzite structure of ZnO has a series of a number of alternating planes which are made of tetrahedral coordinated O^{2-} and Zn^{2+} ions, piling up along the *c*-axis [19]. The ions create positively charged (0001)-Zn and negatively charged (000-1)-O polar surfaces as shown in the inset of Fig. 1(d) [20]. The incor-

poration of Fe^{3+} into ZnO matrix can produce planar defects along (0001) plane which may reduce the surface energy and result in the quick anisotropic growth along different direction instead of c-axis without affecting the intrinsic polarity of nanostructures. The change of morphology from nanowires to nanorods and then nanoparticles may be due to the reason that polar surfaces tend to minimize their surface area. The electrostatic energy may be reduced by interfacing of (0001)-Zn plane with (0001)-O plane. This interfacing will balance the local polar charges and leads to reduce surface area. In brief, the change in the morphology as a function of doping concentration may be due to the increase of charge carriers of Fe^{3+} to replace Zn^{2+} sites into lattice, the positive charge on c-axis growth plane increases and there is driving force produced by dipole-dipole electrostatics interaction, which hinders the growth along one direction [21].

Figure 2 demonstrates the EDS spectra of Fe doped ZnO nanostructures. The spectra of all samples show
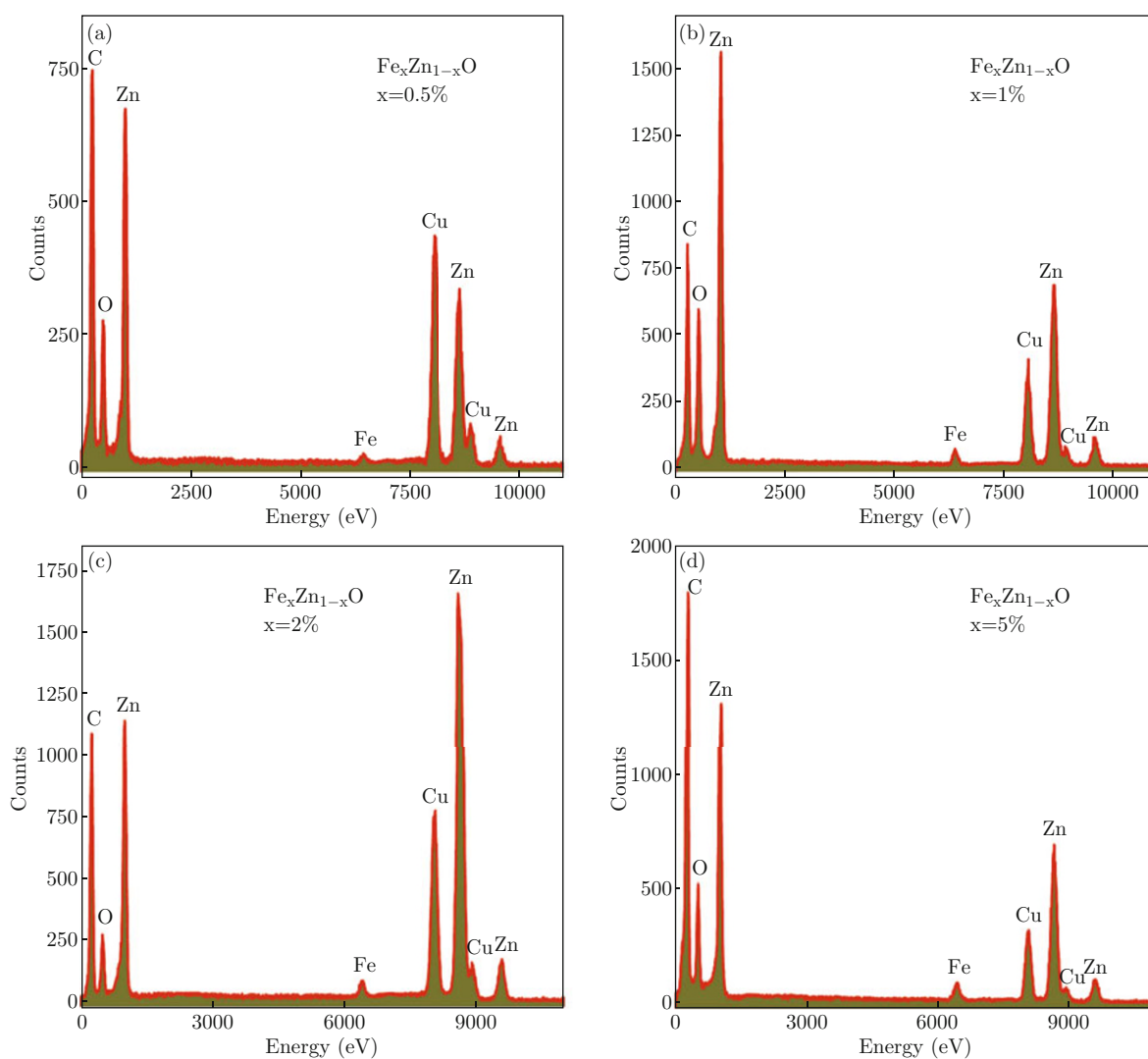
Fig. 2   EDS spectra of Fe doped ZnO Nanostructures.

an obvious presence of Fe dopants and its variation in the concentration into nanostructures. The signals of carbon (C) and copper (Cu) come from the sample grid used for TEM and HRTEM investigations. The statistical analyses over dozen of individual nanowires, nanorods and nanoparticles show that Fe atoms are doped uniformly in the range of x = 0.5∼5% into nanostructures, which are almost consistent with nominal compositions used at the time of chemical reaction during the synthesis process.

Crystal structure and oxidation state

The XRD patterns of $Fe_xZn_{1-x}O$ (x = 0.5%, 1%, 2% & 5%) nanostructures are shown in Fig. 3(a). All the diffraction peaks can be well matched to standard wurtzite structure of ZnO, which confirms single phase crystallinty of the prepared nanostructures. The close view of diffraction patterns in Fig. 3(b) demonstrates two obvious changes as a function of Fe dopant concentration. Firstly, the main diffraction peaks are slightly shifted towards lower angles, which are the results of successful doping [19] due to the small variations in the lattice parameters induced by dopant concentrations. The Rietveld refinement calculations of lattice parameters are tabulated in the Table1. The linear decrease of a-axis and c-axis lattice spacing with increasing concentrations of Fe indicates that the Fe dopants substitute for Zn ions in the lattice, and the decreasing trend can be explained with increase of Fe concentration. There

are many Fe (0.64 Å) ions which can replace Zn (0.74 Å) at octahedral sites of ZnO hexagonal structure, as result there is contraction in the lattice constants. Secondly, it can also be seen in Fig. 3(b) that the width of all peaks is increased with the variation of Fe concentration, which is due to preferred growth of crystal direction and changing in the grain size as different morphologies observed in the above electron microscopic investigations.

In addition, it is interesting to note that the intensity ratio of (002) polar plane to (100) non-polar plane $(I_{(002)}/I_{(100)})$ is remarkably enhanced with the morphological changes (having the following order Nanowires < Nanorods & Nanoparticles) as shown in Fig. 3(b) and given in Table 1. A high ratio of $I_{(002)}/I_{(100)}$ with Fe doping shows a large fraction of polar planes, which clearly demonstrates that the polarization plays an important role for the growth direction [22]. The absence of any extra peak further rules out the formation of secondary phases and in-corroborates well with the HRTEM and SAED results for single phase crystallinty.

XPS is a surface chemical analysis technique that can be used to study the oxidation state and the concentration of elements present in the material. XPS spectra of Fe dopant for all samples have been recorded and typical spectra for x = 0.5 and 5% are displayed in Fig. 4 (a & b). All samples exhibit same spectrum pattern with error of ± 0.2 eV, in which Fe $2p_{3/2}$ and Fe $2p_{1/2}$ peaks are positioned at 724.9 and 710.5 eV, respectively. The peaks positions are different from metallic Fe peak (Fe

Table 1   The Rietveld refinement calculations of lattice parameters.

x(%)	Morphology	Lattice Parameters			$I_{(002)}/I_{(100)}$	Band-gap (nm)	Magnetic Parameters	
		a=b (Å)	c (Å)	V (Å³)			M_s (emu/g)	H_c (Oe)
0	Nanowires	3.2509	5.2069	55.03	0.79	380	—	—
0.5	Nanowires	3.2464	5.2044	54.85	0.91	388	0.02	9
1	Nanorods	3.2439	5.2028	54.75	1.09	392	0.07	11
2	Nanorods + Nanoparticles	3.2420	5.2012	54.67	1.12	407	0.20	139
5	Nanoparticles	3.2401	5.1985	54.58	1.02	443	1.5	261
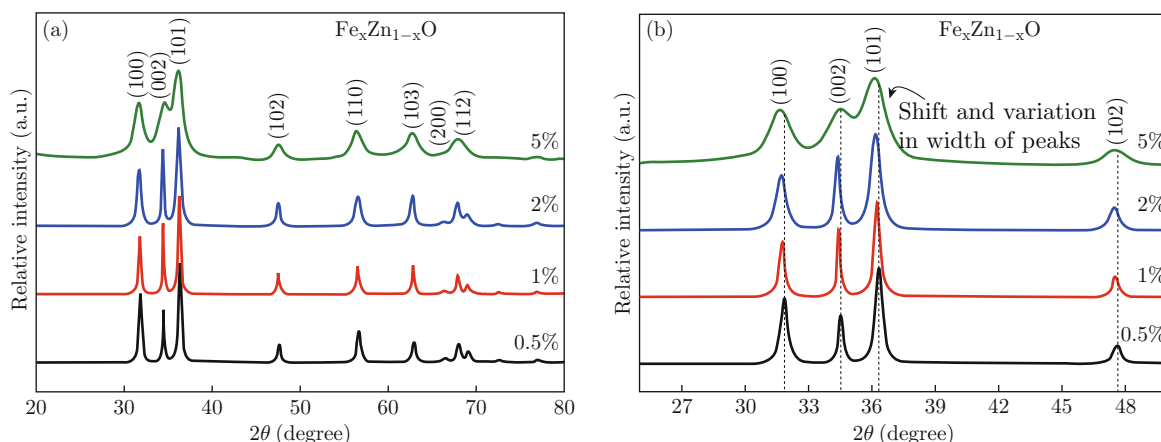
Fig. 3   (a) Full and (b) Extended XRD patterns of $Fe_xZn_{1-x}O$ Nanostructures.
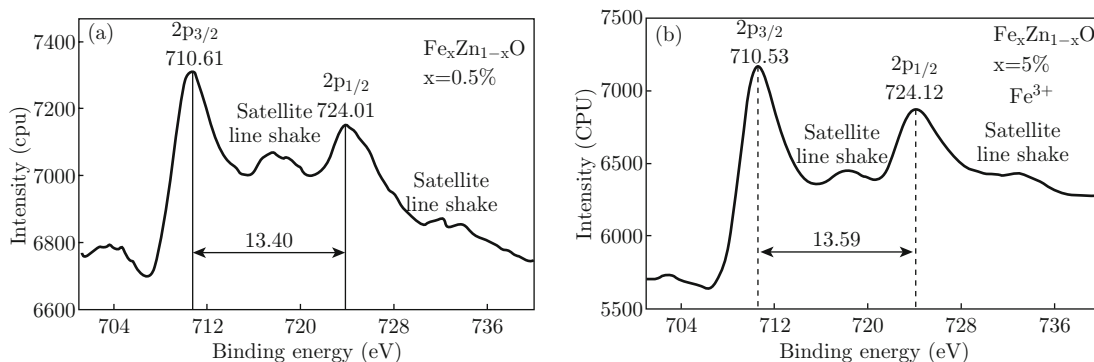
Fig. 4   Oxidation states of Fe dopants in ZnO Nanostructures.
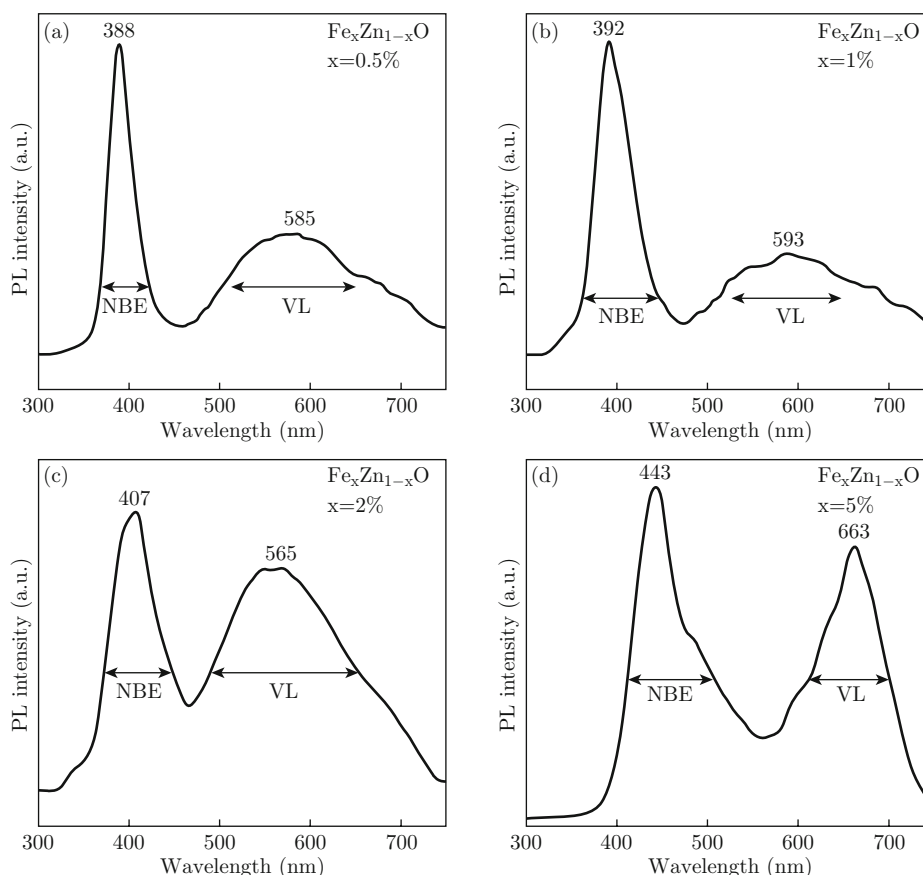
Fig. 5   Room temperature PL of Fe (x=0.5%, 1%, 2% and 5%) doped ZnO Nanostructures.

$2p_{1/2}$ = 719.9 eV & Fe $2p_{3/2}$ = 706.5 eV) and FeO (Fe $2p_{1/2}$ = 722.3 eV & Fe $2p_{3/2}$= 709.3 eV) [23,24]. The existence of satellite lines (S_1 and S_2) suggests that the Fe is incorporated into the ZnO and is in Fe^{3+} valence state for all samples [25]. The concentration of Fe dopants in ZnO is in well agreement with EDS measurements and nominal compositions.

Photoluminescence and ferromagnetic properties

In order to see the Fe doping induced effects on the optical properties of ZnO, the PL spectra have been carried out and are shown in the Fig. 5. The pure ZnO has two emission peaks in UV (380 nm) and visible luminescence (VL) (524 nm) regions of the spectrum. The peak in UV is attributed to near band edge (NBE) transition due to interaction of exciton-exciton through collision process, while in VL usually called green emission band is assigned to the defects (such as singly ionized oxygen vacancy and Zn interstitial defects) [26,27]. The results for Fe doping demonstrate that the NBE and VL are strongly influenced from the amount of Fe doping as shown in Fig. 5 and given in Table 1. It has been interestingly found that NBE of ZnO shows a red shift of about 8, 12, 27 and 63 nm

in the band gap from that of pure ZnO nanowires for 0.5%, 1%, 2% and 5%, respectively. The shift in the UV peak positions illustrates that the Fe doping can significantly tailor the electronic structure and band-gap of ZnO nanostructures. The red shift observed in the band gap of Fe doped ZnO nanoparticles is highest up to recent reported and makes this material potential for the proposed visible light (solar) photocatalyst to overcome the environmental pollution. The red-shift in band gap is usually pretended to the formation of impurity states near the bottom of conduction band of ZnO. The merging of these states with conduction band gives rise to resultant unoccupied orbital bands [28,29]. The increase in the NBE red-shift to visible range can be understood on the basis of change in the morphology through Fe doping. The observed red-shift in the band gap may be due to strong exchange interaction present among d electrons of Fe, and the s and p electrons of ZnO as described in the growth of nanocrystal. These strong exchange interactions among d electrons of ions and sp carriers are most typical feature of DMSs. It has been found that with the increasing Fe doping, the sp-d exchange interaction becomes more dominant due to doping of more d electrons and the difference of Pauling's electronegativity of Fe (1.83) and Zn (1.65). The exchange interactions between electron-

electron and electron-impurity give rise to a negative and a positive correction to the energy of conduction and valance bands, respectively, and lead to reduce the band gap of Fe doped ZnO [27]. The presence of VL band for all doped samples in the PL spectra shows the existence of defects (oxygen vacancy, Zn interstitials and surface defects etc) in the band structure of ZnO.

Figure 6 shows the M-H curves of 0.5%, 1%, 2% and 5% Fe-doped ZnO at room-temperature. The samples with low compositions of 0.5% and 1% exhibit both ferromagnetic and paramagnetic behaviors; while for 2% and 5% samples, there are obvious hysteresis loops. It is noteworthy that the magnetic moment (M_s), remanence (M_r) and coercivity (H_c) are significantly increased with Fe doping concentration in ZnO nanostructures as shown in Fig. 6 and given in Table 1.

The exact origin of room temperature ferromagnetism (FM) in TM doped ZnO is not yet very clear and there are many conflicting reports about it. At this moment, the origin of the FM has usually been explained by several hypotheses: double exchange, super-exchange, direct exchange, carrier mediated exchange interactions, role of anisotropy, oxygen vacancy, bound magnetic polaron overlapping and long-range exchange interactions (RKKY) etc [30-33]. In this mechanism,
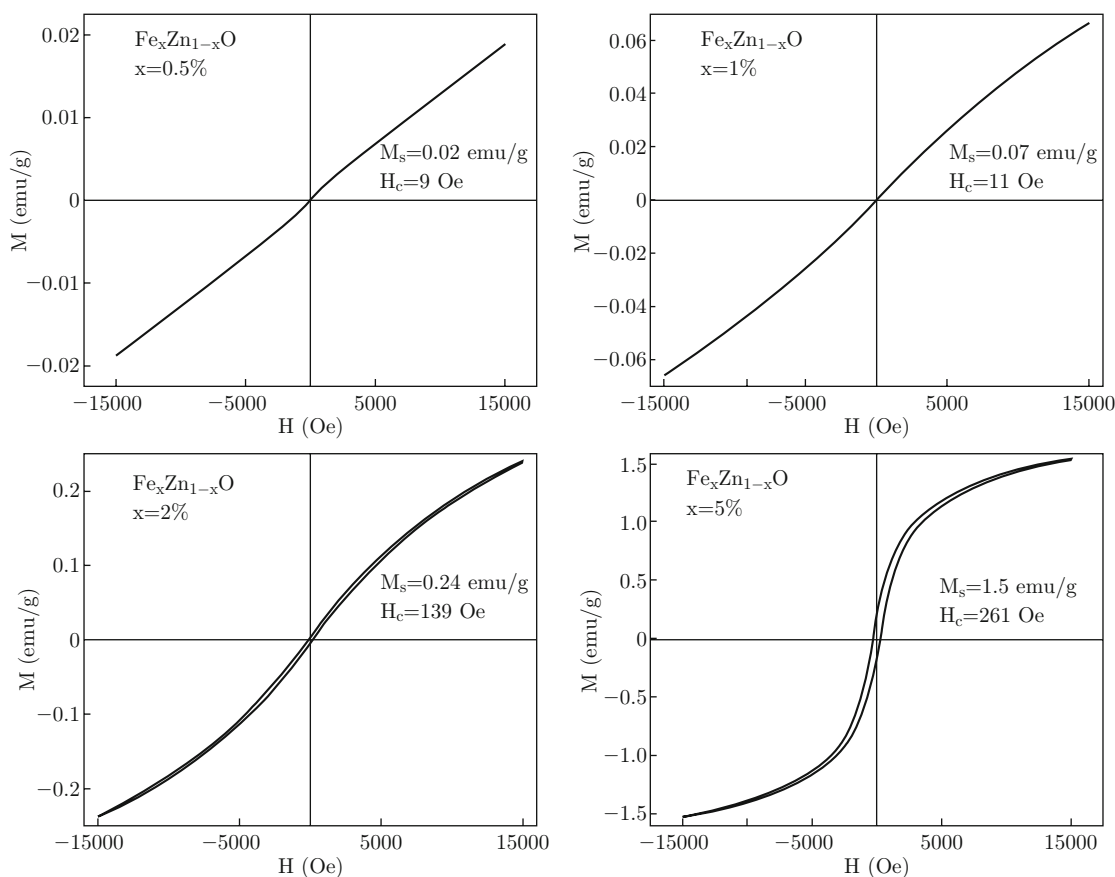
Fig. 6   Field dependent magnetization of Fe doped ZnO Nanostructures.

role of defects (such as oxygen vacancy and zinc interstitial) is mostly considered to be an important for the observed FM in TM doped ZnO [34]. As it is clear from the above morphology and PL results that *sp-d* exchange interactions and presence of defects are increased with increasing Fe concentration, which may be responsible for the origin of observed FM in Fe doped ZnO nanostructures. Moreover, it has been reported that grain boundaries and grain sizes also play a significant role in the ferromagnetic properties of TM doped ZnO [35]. The ferromagnetic behavior of Fe doped ZnO is believed to be more prominent, if it is comprised of nano-grains [36]. Furthermore, it has been reported that Fe doped ZnO samples exhibit ferromagnetic behavior only if containing certain minimum amount of grain boundaries. The amount of grain boundaries is strongly dependent on Fe concentration in the host matrix [36]. Hence, the ferromagnetic behavior of the prepared nanostructures may also be due to smaller grain sizes of the samples and presence of grain boundaries.

Effect of Fe doping on ZnO nanostructures cytotoxicity and ROS production

The bio-compatibility of the prepared nanostructures has been examined on the human cell line (SH-SY5Y cells). The cells have been cultured in Dulbecco's Modification of Eagle's Medium (DMEM) with 10% Fetal Bovine Serum (FBS). These cells have been treated with ZnO nanostructures doped with different Fe concentrations (0.5, 1, 2, 3, 5%) and incubated for 24 hours at 37℃. The effects on the cells have been studied. In order to determine the influence of the synthesized nanostructures on cell viability; CCK-8 analysis has been performed along with phase contrast microscopy to quantify the total number of cells with and without prepared nanostructures. It is depicted in Fig. 7(a) that the prepared nanostructures have no significant effect on the viability of the tested cells. From Fig. 7(b), it is clear that 0.5% Fe doped ZnO nanostructures has no effect on the SH-SY5Y cell viability. With the higher concentration of Fe dopant, the viability of SH-SY5Y cells is slightly affected by ZnO nanostructures, but all the prepared nanostructures may be thought as non toxic towards SH-SY5Y due to very low proportion of damage.

The toxicity of the prepared nanostructures has been further examined by reactive oxygen species (ROS) generation analysis. ROS generation is considered as the main mechanism through which nanomaterials cause damage to the healthy cells. It is generated on the surfaces of the nanomaterials because of the electronic properties of the material. Furthermore, ROS can be generated by the obstructed electronic transport in the
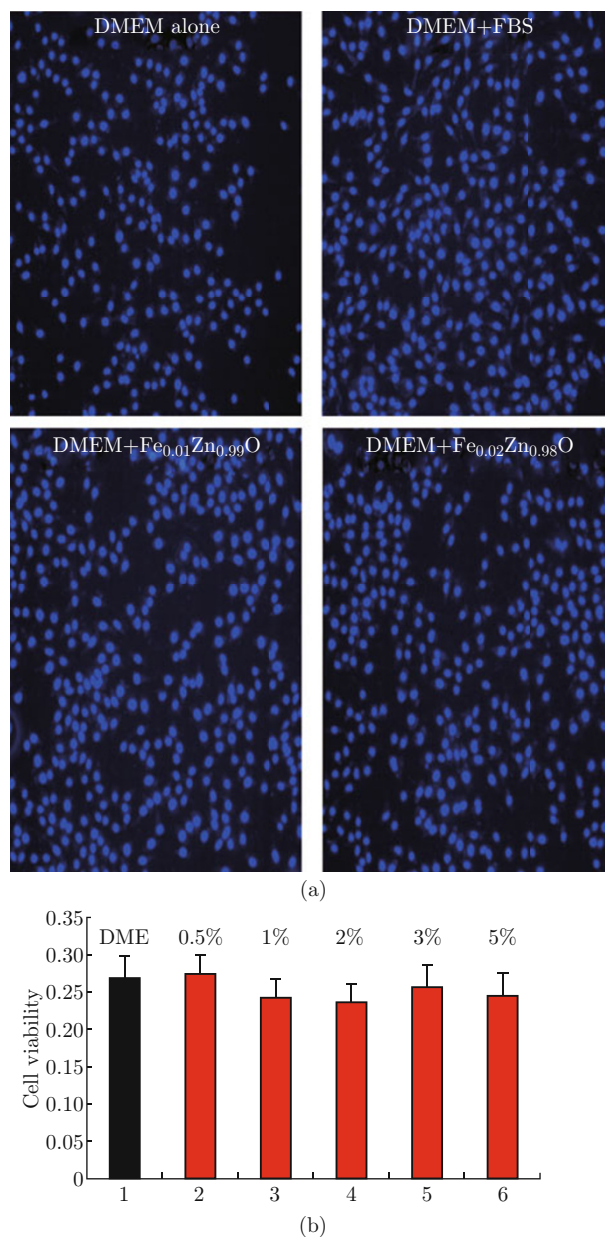
Fig. 7 (a) Florescence Microscope images of untreated and treated cell cultures. (b) Cell viability test as function of ZnO nanostructures doped with various concentrations of Fe.
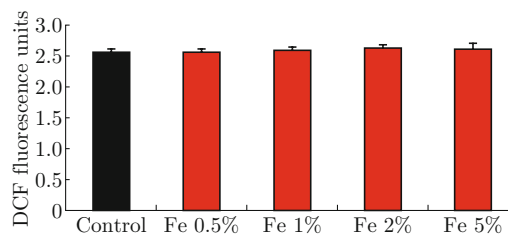
Fig. 8 Effect of Fe doped ZnO nanostructures on the ROS generation in SH-SY5Y Cells.

mitochondrial inner membrane [37]. The elevated generation of ROS can lead to damage cell membrane and

cell which causes cell death [37]. ROS generation has been investigated by Flow cytometry. The cell permeable DCFH-DA dye has been used to know about the oxidative stress in cells [37]. Figure 8 depicts that a negligible amount of ROS produced in SH-SY5Y cells treated with ZnO nanostructures doped with different Fe concentrations (0.5, 1, 2 and 5%).

Conclusions

In conclusion, Fe is successfully doped up to 5% into ZnO lattice using reproducible low-temperature simple, quick and versatile synthesis approach. The investigations reveal that the doping concentration plays a very important role to tune the growth direction of nanocrystal, band gap transitions and FM of nanomaterials. The results appear interesting in the light of the proposed possibilities for the shift of ZnO band gap to represent an alternative of TiO_2 for solar light activated photocatalyst, magneto optical and solar cells devices for the innovative technological applications. It is concluded that Fe doping in ZnO does not change very much the cell viability and ROS production. It is also revealed that Fe doped ZnO is biosafe and biocompatible material for SH-SY5Y Cells.

Acknowledgment

References

[1] H. Zhu, J. Iqbal, H. Xu and D. Yu, "Raman and photoluminescence properties of highly Cu doped ZnO nanowires fabricated by vapor-liquid-solid process", J. Chem. Phys. 129(12), 124713 (2008). http://dx.doi.org/10.1063/1.2981050

[2] P. V. Radovanovic and D. R. Gamelin, "High-temperature ferromagnetism in Ni_2-doped ZnO aggregates prepared from colloidal diluted magnetic semiconductor quantum dots", Phys. Rev. Lett. 91(15), 157202 (2003). http://dx.doi.org/10.1103/PhysRevLett.91.157202

[3] Z. L. Wang, "Zinc oxide nanostructures: growth, properties and applications", J. Phys: Condens. Matter. 16, 829-858 (2004). http://dx.doi.org/10.1088/0953-8984/16/25/R01

[4] H. T. Ng, J. Han, T. Yamada, P. Nguyen, Y. P. Chen and M. Meyyappan, "Single crystal nanowire vertical surround-gate field-effect transistor", Nano Lett. 4(7), 1247-1252 (2004). http://dx.doi.org/10.1021/nl049461z

[5] C. Soci, A. Zhang, B. Xiang, S. A. Dayeh, D. P. R. Aplin, J. Park, X. Y. Bao, Y. H. Lo and D. Wang, "ZnO nanowire UV photodetectors with high internal gain", Nano Lett. 7(4), 1003-1009 (2007). http://dx.doi.org/10.1021/nl070111x

[6] Q. H. Li, Y. X. Liang, Q. Wan and T. H. Wang, "Oxygen sensing characteristics of individual ZnO nanowire transistors", Appl. Phys. Lett. 85(26), 6389-6391 (2004). http://dx.doi.org/10.1063/1.1840116

[7] C. J. Lee, T. J. Lee, S. C. Lyu, Y. Zhang, H. Ruh and H. J. Lee, "Field emission from well-aligned zinc oxide nanowires grown at low temperature", Appl. Phys. Lett. 81(19), 3648-3650 (2002). http://dx.doi.org/10.1063/1.1518810

[8] M. H. Huang, S. Mao, H. Feick, H. Yan, Y. Wu, H. Kind, E. Weber, R. Russo and P. Yang, "Room-temperature ultraviolet nanowire nanolasers", Science 292(5523), 1897-1899 (2001). http://dx.doi.org/10.1126/science.1060367

[9] X. D. Wang, J. H. Song, J. Liu and Z. L. Wang, "Direct-current nanogenerator driven by ultrasonic waves", Science 316(5821), 102-105 (2007). http://dx.doi.org/10.1126/science.1139366

[10] B. Dindar and S. Icli, "Unusual photoreactivity of zinc oxide irradiated by concentrated sunlight", J. Photochem. Photobiol. A: Chem. 140(3), 263-268 (2001). http://dx.doi.org/10.1016/S1010-6030(01)00414-2

[11] M. A. Behnajady, N. Modirshahla and R. Hamzavi, "Kinetic study on photocatalytic degradation of CI Acid Yellow 23 by ZnO photocatalyst", J. Hazard. Mater. 133(1), 226-232 (2006). http://dx.doi.org/10.1016/j.jhazmat.2005.10.022

[12] S. V. Bhat and F. L. Deepak, "Tuning the bandgap of ZnO by substitution with Mn^{2+}, Co^{2+} and Ni^{2+}", Solid State Comm. 135(6), 345-347 (2005). http://dx.doi.org/10.1016/j.ssc.2005.05.051

[13] T. Dietl, H. Ohno, F. Matsukura, J. Cibert and D. Ferrand, "Zener model description of ferromagnetism in Zinc-Blende magnetic semiconductors", Science 287(5455), 1019-1022 (2000). http://dx.doi.org/10.1126/science.287.5455.1019

[14] Quarta, R. Di Corato, L. Manna, S. Argentiere, R. Cingolani, G. Barbarella and T. Pellegrino, " Multifunctional nanostructures based on inorganic nanoparticles and oligothiophenes and their exploitation for cellular studies", J. Am. Chem. Soc. 130(32), 10545-10555 (2008). http://dx.doi.org/10.1021/ja800102v

[15] Morfesis, D. Fairhurst, NSTI Nanotechnology Conference and Trade Show. NSTI Nanotech Anaheim, CA May 8-12, (2005).

[16] W. J. Rasmussen, E. Martinez, P. Louka, and D. G. Wingett, "Zinc oxide nanoparticles for selective destruction of tumor cells and potential for drug delivery applications", Expert Opin. Drug Deliv. 7(9), 1063-1077, (2010). http://dx.doi.org/10.1517/17425247.2010.502560

[17] Rita John and Rajaram Rajakumari, "Synthesis and characterization of rare earth ion doped nano ZnO", Nano Micro Lett. 4(2), 65-72 (2012). http://dx.doi.org/10.3786/nml.v4i2.p65-72

[18] J. Iqbal, B. Wang, X. F. Liu, H. Be, D. P. Yu and R. H. Yu, "Oxygen-vacancy-induced green emission and room-temperature ferromagnetism in Ni-doped ZnO nanorods", New Journal Phys. 11(6), 063009 (2009). http://dx.doi.org/10.1088/1367-2630/11/6/063009

[19] Y. J. Li, C. Y. Wang, M. Y. Lu, K. M. Li and L. J. Chen, "Electrodeposited hexagonal ring-like superstructures composed of hexagonal Co-doped ZnO nanorods with optical tuning and high-temperature ferromagnetic properties", Cryst. Growth Des. 8(8), 2598-2602 (2008). http://dx.doi.org/10.1021/cg7007864

[20] X. Y. Kong, Y. Ding, R. Yang and Z. L. Wang, "Single-crystal nanorings formed by epitaxial self-coiling of polar nanobelts", Science 303(5662), 1348-1351 (2004). http://dx.doi.org/10.1126/science.1092356

[21] Z. Y. Tang, N. A. Kotov and M. Giersig, "Spontaneous organization of single CdTe nanoparticles into lumines-cent nanowires", Science 297(5579), 237-240 (2002). http://dx.doi.org/10.1126/science.1072086

[22] J. M. D. Coey, M. Viret and S. von Molnar, "Mixed-valence manganite", Adv. Phys. 48(2), 167-293 (1999). http://dx.doi.org/10.1080/000187399243455

[23] G.R. Li, T. Hu, G. L. Pan, T. Y. Yan, X. P. Gao and H. Y. Zhu, "Morphology- function relationship of ZnO: polar planes, oxygen vacancies, and activity", J. Phys. Chem. C 112(31), 11859-11864 (2008). http://dx.doi.org/10.1021/jp8038626

[24] S. Baek, J. Song and S. Lim, "Improvement of the op-tical properties of ZnO nanorods by Fe doping", Physica B 399(2), 101-104 (2007). http://dx.doi.org/10.1016/j.physb.2007.05.030

[25] J. F. Moulder, William F. Stickle, Peter E. Sobol and Kenneth D. Bomben "Handbook of X-ray photoelec-tron spectroscopy", Perkin Elmer Corporation, 84-85, (1992).

[26] Y. W. Chen, Y. C. Liu, S. X. Lu, C. S. Xu, C. L. Shao, C. Wang, J. Y. Zhang, Y. M. Lu, D. Z. Shen and X. W. Fan, "Optical properties of ZnO and ZnO: in nanorods assembled by sol-gel method", J. Chem. Phys. 123(13), 134701 (2005). http://dx.doi.org/10.1063/1.2009731

[27] A. B. Djurisic, W. C. H. Choy, V. A. L. Roy, Y. H. Leung, C. Y. Kwong, K. W. Cheah, T. K. Gundu Rao, W. K. Chan, H. Fei Lui and C. Surya, "Photo-luminescence and electron paramagnetic resonance of ZnO tetrapod structures", Adv. Funct. Mater. 14(9), 856-864, (2004). http://dx.doi.org/10.1002/adfm.200305082

[28] W. Li, Y. Wang, H. Lin, S. Ismat Shah, C. P. Huang, D. J. Doren, S. A. Rykov, J. G .Chen and M. A. Barteau, "Band gap tailoring of Nd^{3+} -doped TiO_2 nanoparticles", Appl. Phys. Lett. 83(20), 4143-4145 (2003). http://dx.doi.org/10.1063/1.1627962

[29] J. Iqbal, X. Liu and H. Zhu, "Trapping of Ce elec-trons in band gap and room temperature ferromag-netism of Ce^{4+} doped ZnO nanowires", J. Appl. Phys. 106(8), 083515-083515-6 (2009). http://dx.doi.org/10.1063/1.3245325

[30] S. J. Pearton, W. H. Heo, M. Ivill, D. P. Norton and T. Steiner, "Dilute magnetic semiconducting oxides", Semicond. Sci. Technol. 19(10), 54-59 (2004). http://dx.doi.org/10.1088/0268-1242/19/10/R01

[31] M. Venkatesan, C. B. Fitzgerald, J. G. Lun-ney and J. M. D. Coey, "Anisotropic ferromag-netism in substituted zinc oxide", Phys. Rev. Lett. 93(17), 177206 (2004). http://dx.doi.org/10.1103/PhysRevLett.93.177206

[32] M. Venkatesan, C. B. Fitzgerald and J. M. D. Coey, "Thin films: unexpected magnetism in a dielectric ox-ide", Nature 430(7000), 630-630 (2004). http://dx.doi.org/10.1038/430630a

[33] N. Khare, M. J. Kappers, M.Wei, M.G. Blamire and J. L. Macmanus-Driscoll, "Defect-induced fer-romagnetism in Co-doped ZnO", Adv. Mater. 18(11), 1449-1452 (2006). http://dx.doi.org/10.1002/adma.200502200

[34] B. B. Straumal, S. G. Protasova, d, A. A. Mazilkin, G. Schütz, E. Goering, B. Baretzky and P. B. Straumal, "Ferromagnetism of zinc oxide nanograined films", JETP Letters. 97(6), 367-377 (2013). http://dx.doi.org/10.1134/S0021364013060143

[35] B. B. Straumal, S. G. Protasova, A. A. Mazilkin, T. Tietze, E. Goering, G. Schütz, P. B. Straumal and B. Baretzky, "Ferromagnetic behaviour of Fe-doped ZnO nanograined films", Beilstein J. Nanotechnol. 4(1), 361-369 (2013). http://dx.doi.org/10.3762/bjnano.4.42

[36] T. Xia, M. Kovochich, M. Liong, L. Madler, B. Gilbert, H. Shi, J. I. Yeh, J. I. Zink and A. E. Nel, "Comparison of the mechanism of toxicity of zinc oxide and cerium oxide nanoparticles based on dissolution and oxidative stress properties", ACS Nano. 2(10), 2121-2134 (2008). http://dx.doi.org/10.1021/nn800511k

[37] C. Hanley, A. Thurber, C. Hanna, A. Punnoose. J. Zhang and D. G. Wingett, "The influences of cell type and ZnO nanoparticle size on immune cell cy-totoxicity and cytokine induction", Nanoscale Res. Lett. 4(12), 1409-1420 (2009). http://dx.doi.org/10.1007/s11671-009-9413-8